J BONE ONCOL 40 (2023) 100477

Contents lists available at ScienceDirect

Journal of Bone Oncology

journal homepage: www.elsevier.com/locate/jbo

Review Article

Molecular imaging of bone metastasis

Eliana Khojasteh [a], Farrokh Dehdashti [a,b], Monica Shokeen [a,b,c,*]

[a] Edward Mallinckrodt Institute of Radiology, Washington University School of Medicine, St. Louis, MO, USA
[b] Alvin J. Siteman Cancer Center, Washington University School of Medicine, St. Louis, MO, USA
[c] Department of Biomedical Engineering, Washington University in St. Louis, St. Louis, MO, USA

ARTICLE INFO

Keywords:
Molecular imaging
Nuclear imaging
Bone scintigraphy
Bone metastasis
Breast cancer
Prostate cancer
Multiple myeloma

ABSTRACT

Recent advances in molecularly targeted modular designs for in vivo imaging applications has thrusted open possibilities of investigating deep molecular interactions non-invasively and dynamically. The shifting landscape of biomarker concentration and cellular interactions throughout pathological progression requires quick adaptation of imaging agents and detection modalities for accurate readouts. The synergy of state of art instrumentation with molecularly targeted molecules is resulting in more precise, accurate and reproducible data sets, which is facilitating investigation of several novel questions. Small molecules, peptides, antibodies and nanoparticles are some of the commonly used molecular targeting vectors that can be applied for imaging as well as therapy. The field of theranostics, which encompasses joint application of therapy and imaging, is successfully leveraging the multifunctional use of these biomolecules [1,2].

Sensitive detection of cancerous lesions and accurate assessment of treatment response has been transformative for patient management. Particularly, since bone metastasis is one of the dominant causes of morbidity and mortality in cancer patients, imaging can be hugely impactful in this patient population. The intent of this review is to highlight the utility of molecular positron emission tomography (PET) imaging in the context of prostate and breast bone metastatic cancer, and multiple myeloma. Furthermore, comparisons are drawn with traditionally utilized bone scans (skeletal scintigraphy). Both these modalities can be synergistic or complementary for assessing lytic- and blastic- bone lesions.

1. Introduction

Breast [3] and prostate [4] cancer has high propensity to metastasize to bone, which is a significant contributor of morbidity. Multiple myeloma is another cancer that originates in the bone marrow and causes multiple osteolytic lesions in the skeleton [5]. There is an unambiguous negative correlation between bone metastasis and survival [6]; necessitating efficient methods to detect bone metastasis in a timely manner. Advancements in molecular imaging approaches has improved accuracy of diagnosis, staging and therapy response [7–9]. Clinical imaging of bone, including the bone marrow utilizes a spectrum of imaging modalities such as: X-ray based radiological planar and tomographic (computed tomography (CT)) imaging, high-spatial resolution magnetic resonance imaging (MRI), and nuclear imaging (single-photon emission computed tomography (SPECT) and positron emission tomography (PET)). Each of these approaches has its advantages and limitations. It is desirable that the imaging modality is sensitive, specific and able to capture the heterogeneous biology of the disease. Bone metastasis can lead to osteoblastic or osteolytic lesions [10], and multiple myeloma is characterized by diffuse as well as focal spread in the bone marrow, including lytic bone lesions. This review is specifically focused on molecular PET and bone scans for investigating bone metastasis in breast and prostate cancer, and multiple myeloma. Magnetic resonance imaging (MRI) is a modality that provides high spatial resolution in the osseous tissue. However, MRI is beyond the scope of this review and best reviewed elsewhere.

2. Discussion

X-ray based imaging modalities are excellent for evaluation of bone, as the opacity of bone relative to other soft tissues generates considerable contrast. In addition, X-ray based scans are high-throughput, readily available, and overall, well tolerated by the patient. While X-ray based imaging has historically been fundamental for detecting a

* Corresponding author at: Mallinckrodt Institute of Radiology, 510 South Kingshighway Boulevard, St. Louis, MO 63110, USA.
E-mail address: mshokeen@wustl.edu (M. Shokeen).

https://doi.org/10.1016/j.jbo.2023.100477
Received 30 January 2023; Received in revised form 27 March 2023; Accepted 31 March 2023
Available online 5 April 2023

Table 1

Imaging Molecule	Modality	Mechanism of Action
^{18}F-fluorodeoxyglucose (^{18}F-FDG) ^{18}F half-life ($t_{1/2}$): 109.8 min	Positron Emission Tomography (PET) imaging	Glucose metabolism. ^{18}F-FDG targets metabolically active cells including tumor lesions and inflammatory cells.
^{18}F-sodium fluoride (^{18}F-NaF)	PET imaging	Quantification of bone turnover. Radioactive fluoride ion ($^{8}F^{-}$) is incorporated into hydroxyapatite, and its uptake reflects osteoblastic activity and bone perfusion.
Technetium-99 m (^{99m}Tc) complexed to methylene diphosphonate (MDP) (^{99m}Tc-MDP) ^{99m}Tc half-life ($t_{1/2}$): 6 h	Skeletal Imaging (Bone Scintigraphy/ Skeletal Scintigraphy/Bone Scan) ^{99m}Tc is a radionuclide that emits gamma rays, which is used for gamma scintigraphic imaging.	^{99m}Tc-MDP targets bone repair of the bone damaged by cancer metastasis. Broad mechanism of action is chemical adsorption and incorporation into the hydroxyapatite structure.
Technetium-99 m (^{99m}Tc) complexed to hydroxydiphosphonate (HDP) forming ^{99m}Tc-HDP	Skeletal Imaging (Bone Scintigraphy/ Skeletal Scintigraphy/Bone Scan) ^{99m}Tc is a radionuclide that emits gamma rays, which is used for gamma scintigraphic imaging.	Skeletal uptake of technetium ^{99m}Tc-HDP occurs as a function of skeletal blood flow and osteogenic activity associated with malignant bone lesions.
^{11}C-choline ^{11}C half-life ($t_{1/2}$): 20.3 min	PET imaging	Targets high metabolic rate in tumor cells. Choline uptake is increased in tumor cells to keep up with the demands of the synthesis of phospholipids in their cellular membranes.
^{18}F-DCFPyl (Prostate-specific membrane antigen (PSMA) PET)	PET imaging	A urea-based radiotracer composed of the prostate specific membrane antigen (PSMA) targeting agent DCFPyL that images PSMA-expressing tumor cells.
^{99m}Tc-PSMA	Single-photon emission computed tomography (SPECT) imaging	Targets PSMA-expressing tumor cells.
^{18}F-fluciclovine (anti-1-amino-3-18F-fluorocyclobutane-1-carboxylic acid)	PET imaging	^{18}F-Fluciclovine is a synthetic amino acid analog. It targets increased amino acid consumption in prostate cancer cells.
^{89}Zr-trastuzumab(Human epidermal growth factor receptor 2 (HER2) targeted PET) ^{89}Zr half-life ($t_{1/2}$): 3.3 d	PET imaging	Trastuzumab is a humanized monoclonal antibody against HER2. Trastuzumab can be radiolabeled with the positron emitter, Zr-89, for whole body PET imaging

variety of malignant bone lesions primarily based on osteoblastic activity, this modality is not sensitive for capturing molecular events and frequently misses early stage osteoclastic lesions [11]. Nuclear imaging can efficiently fill these gaps by capturing molecular events with high sensitivity [12]. While, here we are covering molecular PET imaging and skeletal scintigraphy (Table 1); we acknowledge additional functional and anatomical modalities such as CT and MRI that play an essential role in evaluating bone metastasis and are covered by other dedicated reviews on these respective modalities [13].

3. Breast cancer

3.1. ^{18}F-FDG-PET in breast cancer

Molecular imaging used in conjunction with conventional imaging, is an increasingly useful modality for phenotyping the heterogeneity in breast cancer at a whole body level [14]. Positron emission tomography (PET) performed with ^{18}F-fluorodeoxyglucose (^{18}F-FDG), a glucose analogue, is widely used for evaluating metastatic disease in a variety of cancers. ^{18}F-FDG-PET measures glucose metabolism, which is upregulated in malignant cells. It remains the clinical tour de force tracer for imaging oncologic patients with high sensitivity and accuracy.

3.2. ^{18}F-FDG-PET/CT for postoperative surveillance

Surveillance of breast cancer patients after primary treatment is important in monitoring and detecting local recurrences and distant metastasis as early as possible [15]. The study by Jung et al compared ^{18}F-FDG-PET/CT with conventional imaging for detection of local recurrence or distant metastasis during postoperative surveillance of patients with stage II or greater breast cancer (1,161 patients) [16]. Conventional imaging included mammography, breast ultrasound, whole-body bone scintigraphy, and chest radiography. Conventional imaging alone had 75.4 % sensitivity, 98.7 % specificity, 93.4 % positive predictive value (PPV), and 94.3 % negative predictive value (NPV). ^{18}F-FDG-PET/CT alone had 97.5 % sensitivity, 98.8 % specificity, 95.4 % PPV, and 99.4 % NPV. Sensitivity of ^{18}F-FDG-PET/CT was significantly higher ($p < 0.05$) than the sensitivity of conventional imaging. Conventional imaging and ^{18}F-FDG-PET/CT combined had 98.6 % sensitivity, 98.2 % specificity, 96.7 % PPV, and 99.7 % NPV. Though the combination of conventional imaging and ^{18}F-FDG-PET/CT showed improvements, the combined results were not significantly different ($p = 0.43$) from the results of ^{18}F-FDG-PET/CT alone. Additionally, ^{18}F-FDG-PET/CT yielded less false positive (17 vs 19) and false negative results (9 vs 88) than conventional imaging. The limitations of this study included non-uniform use of follow-up imaging methods and the imaging interval. In addition, this study focused on late-stage breast cancer patients rather than early-stage breast cancer patients and not all PET/CT-positive or conventional imaging-positive lesions were histopathologically confirmed. The results ultimately suggest that ^{18}F-FDG-PET/CT serves as a highly sensitive and effective imaging modality for postoperative surveillance of breast cancer patients.

3.3. ^{18}F-FDG-PET/CT versus bone scintigraphy in breast cancer

Bone scintigraphy is the conventional method used to detect bone metastases in oncologic patients. Also referred to as skeletal scintigraphy or bone scan, this is a common nuclear medicine modality that widely uses the radionuclide Technetium-99m (^{99m}Tc) complexed to a diphosphonate, either methylene diphosphonate (MDP) forming ^{99m}Tc-MDP or hydroxydiphosphonate (HDP) forming ^{99m}Tc-HDP for SPECT scan [17].

Van Es et al compared ^{18}F-FDG PET with ^{99m}Tc bone scintigraphy for clinical management of metastatic breast cancer [18]. They retrospectively compared management recommendations based on bone lesion assessment by ^{18}F-FDG PET plus contrast-enhanced CT or bone

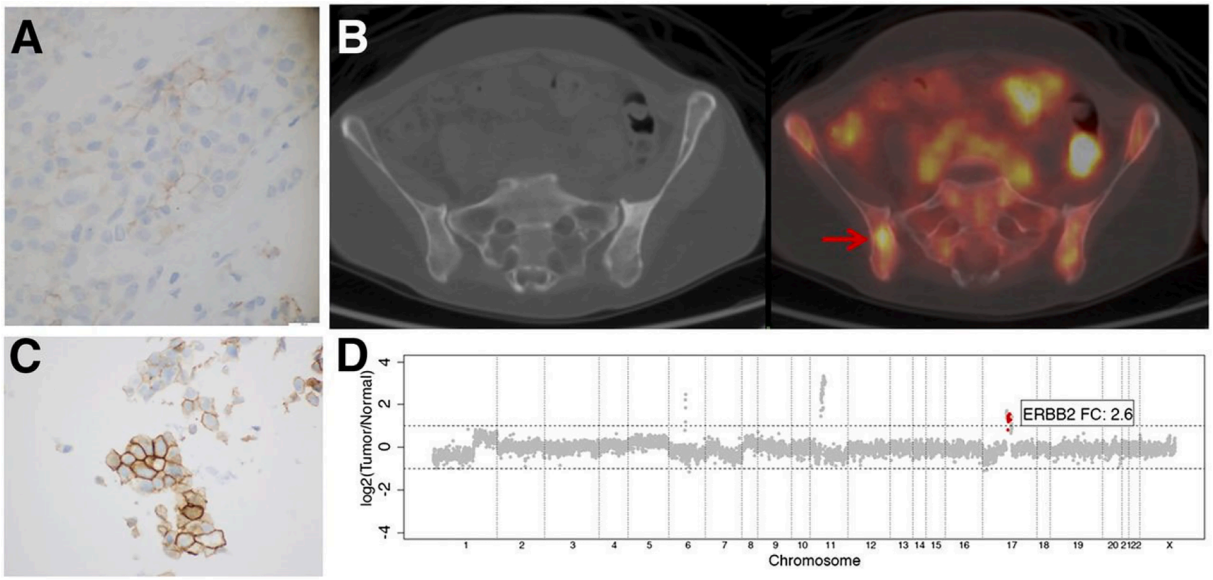

Fig. 1. 38-year-old woman with primary ER-positive/HER2-negative invasive ductal breast carcinoma. (A) Immunohistochemistry score of primary breast malignancy was 1+ (at × 400 magnification), consistent with HER2-negative malignancy. (B) Axial CT and ^{89}Zr-trastuzumab PET/CT demonstrated ^{89}Zr-trastuzumab avidity in right ilium (arrow, SUVmax of 5.9). Avidity in bowel is considered physiologic. (C) Biopsy of right ilium demonstrated metastatic breast carcinoma with equivocal immunohistochemistry score of 2+ (at × 400 magnification). (D) MSK-IMPACT copy-number plot demonstrating HER2 amplification. Each dot represents probe set, and values on y-axis show log2-transformed ratio of tumor vs normal. ERBB2 change was 2.6-fold, consistent with HER2-positive disease. Originally published in JNM [Ref 24].

scintigraphy plus contrast-enhanced CT, for patients with newly diagnosed, non-rapidly progressive metastatic breast cancer of all subtypes. All scans were performed shortly before the start of first-line therapy. In all 102 patients but five, metastatic breast cancer was pathologically proven by histologic biopsy mostly from a bone metastatic site. In total, 3,473 unequivocal bone lesions were identified in 102 evaluated patients (39 % by contrast-enhanced CT, 26 % by bone scintigraphy, and 87 % by ^{18}F-FDG PET). Additional bone lesions on ^{18}F-FDG PET plus contrast-enhanced CT compared with bone scintigraphy plus contrast-enhanced CT led to change in metastatic breast cancer (MBC) management recommendations in 16 % of patients (95 % CI, 10 %–24 %). Bone scintigraphy also changed management compared with ^{18}F-FDG PET in one patient (1 %; 95 % CI, 0 %–5%). In 26 % (95 % CI, 19 %–36 %) of patients, an additional ^{18}F-FDG PET study was requested, because bone scintigraphy provided insufficient information. Overall, these data supported the use of ^{18}F-FDG PET as a primary imaging modality for assessment of bone lesions in newly diagnosed metastatic breast cancer.

3.4. ^{18}F-FDG PET versus ^{18}F-NaF PET in breast cancer

A positron-emitting radiopharmaceutical that is used to image bones is ^{18}F-sodium fluoride (^{18}F-NaF) [19,20]. ^{18}F-NaF has near perfect single pass retention in the bone and is rapidly cleared from plasma in a biexponential manner. Its osseous uptake is due to chemisorption with exchange of ^{18}F ion for OH ion on the surface of the hydroxyapatite matrix of bone forming fluoroapatite and then migration of ^{18}F ion into the crystalline matrix of bone. Its binding to serum protein is minimal and is rapidly cleared through genitourinary tract resulting in quality images with high bone-to-background ratio in a shorter time [21]. The significance of synergistic evaluation of ^{18}F-FDG PET and ^{18}F-NaF PET for predicting time to skeletal-related events (tSRE), time to progression (TTP), and survival in patients with bone-dominant metastatic breast cancer is discussed in a prospective study by Peterson et al. [22]. Authors of the study emphasize the need for accurate assessment of bone-dominant metastatic breast cancer for improving the use of systemic therapies in this patient population. Recognized limitations of bone scintigraphy involve longer time to detect response, and the inability to differentiate between progression and bone healing related flare from effective therapy. Partly due to these ambiguities, RECIST 1.1 does not include bone metastasis as a measurable site of response [23]. This study evaluated both serial ^{18}F-NaF PET and ^{18}F-FDG PET to predict tSRE, TTP, and overall survival (OS) prospectively in patients with bone-dominant metastatic breast cancer starting new systemic therapy. The guiding hypothesis was that serial ^{18}F-FDG PET and ^{18}F-NaF PET would provide complementary measures of activity of breast cancer bone metastases, and that each might predict response to therapy. The study involved baseline ^{18}F-FDG PET and ^{18}F-NaF PET (scan1) that were completed before initiation of new systemic therapy. Follow-up ^{18}F-FDG PET and ^{18}F-NaF PET (scan2) were completed at the discretion of the treating physician following therapy. Because the average ^{18}F-FDG uptake in bone versus soft-tissue metastases is low, the study included Modified PET Response Criteria in Solid Tumors (mPERCIST) using a lean body mass adjusted standardized uptake (SUL_{peak}) greater than 1.5 × the value of normal liver. The study found that patients with metabolic response (CR, PR, and stable disease) experienced significant prolongation in tSRE (47.6 vs 4.6 mo) and TTP (14.1 vs 3.8 mo). ^{18}F-FDG PET uptake changes assessed by mPERCIST were strongly associated with clinical outcomes of interest.

3.5. Human epidermal growth factor receptor 2 (HER2) PET in breast cancer

A paradigm shift in the imaging agent design has been introduced with the use of antibodies as targeting vectors. Imaging agents based on intact antibodies and antibody fragments are uniquely specific for their targets, which confers high signal to background. Human epidermal growth factor receptor 2 (HER2) is a biomarker of breast cancer whose expression could guide precision therapies. For example, breast cancer patients with HER2-positive malignancies can receive HER2-targeted therapy that is a more effective treatment in this group of patients. It is important to note that HER2-positive metastases can still occur in patients with HER2-negative primary breast cancer. Paradoxically, not all patients with HER2-positive disease respond to HER2-targeted therapy. This has been attributed in part to the limitations of tissue

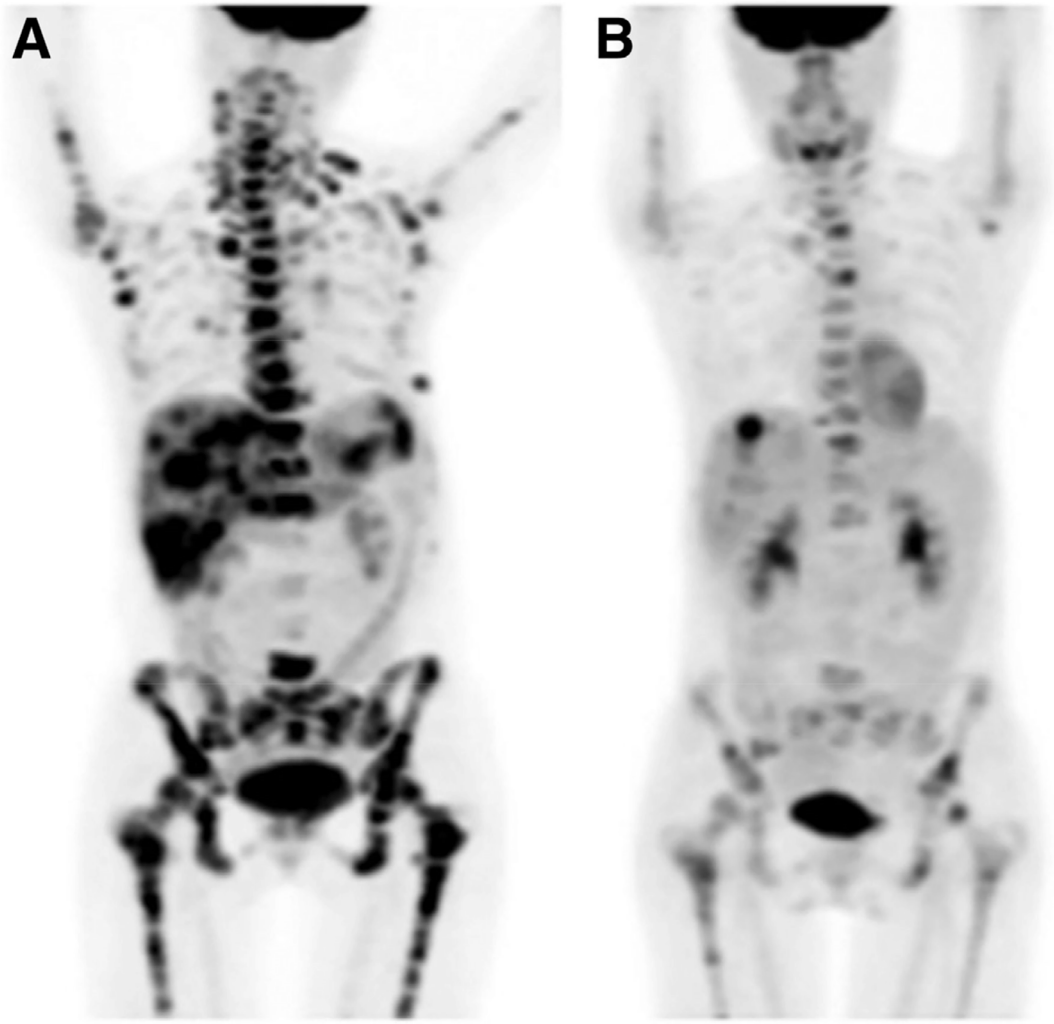

Fig. 2. Patient from Fig. 1 underwent HER2-targeted therapy after biopsy had demonstrated HER2 amplification in osseous metastasis. Maximum-intensity projections from ^{18}F-FDG PET/CT studies before (A) and after (B) 3 mo of systemic treatment including trastuzumab and pertuzumab demonstrate treatment response. Originally published in JNM [Ref 24].

biopsy and in vitro assays in detecting the HER2 status considering breast cancer heterogeneity. In addition, HER2 status can change during the course of disease. Ulaner et al evaluated whether imaging with a HER2-targeted PET tracer could detect HER2-positive metastases in patients with HER2-negative primary breast cancer [24]. The study examined nine patients, all of whom were confirmed to have HER2-negative primary breast cancer. Molecular PET using ^{89}Zr-trastuzumab, a radiolabeled HER-2 monoclonal antibody, demonstrated potential sites of HER2-positive metastases in five patients (3 had bone metastasis) and biopsy confirmed HER2-positive metastases in two of these five patients. In the other three patients, there was no evidence to suggest the presence of HER2-positive metastases, and ^{89}Zr-trastuzumab PET/CT results were classified as false positive. One of the study subjects, with pathologically demonstrated ER-positive/HER2-negative primary invasive ductal carcinoma (Fig. 1**A**), when imaged with ^{89}Zr-trastuzumab PET/CT demonstrated multiple suggestive osseous foci (Fig. 1**B**). The most avid foci were in the right ilium and right proximal femur (SUVmax, 5.9). Biopsy of the right ilium demonstrated equivocal HER2 findings. The immunohistochemistry results were equivocal (Fig. 1**C**) because of incomplete membranous staining in a small percentage of the cells. Given the equivocal results, further testing was performed with the MSK-IMPACT assay [25]. The change in ERBB2 on MSK-IMPACT was 2.6-fold (Fig. 1**D**) [25]. Therefore, this ^{89}Zr-trastuzumab focus was considered true-positive for a HER2-positive distant metastasis [26]. The patient was then switched to treatment with trastuzumab, pertuzumab, and docetaxel and was followed up with ^{18}F-FDG PET/CT, which showed a decrease in the size and ^{18}F-FDG avidity of the liver and nodal metastases, as well as a decrease in the ^{18}F-FDG avidity of the osseous lesions, representing a partial response to treatment (Fig. 2**A and 2B**). The results indicate that despite the small sample size ^{89}Zr-trastuzumab PET/CT has the potential to play a vital role in detecting HER2-positive metastases in patients with HER2-negative primary breast cancer, ultimately allowing these patients to receive critical life-lengthening treatment. Moving forward, HER2-targeted imaging may be beneficial in determining whether HER2-negative primary breast cancer patients could benefit from HER2-targeted therapy.

4. Prostate cancer

4.1. ^{18}F-sodium fluoride PET versus bone scintigraphy

Overall, ^{18}F-NaF [27] PET/CT has shown to be superior to ^{99m}Tc-based tracers in detection of osseous metastatic disease. Apolo et al demonstrated that ^{18}F-NaF PET/CT successfully detected more bone lesions than conventional bone scintigraphy (^{99m}Tc-MDP) in 69 % of patients [28]. Conventional bone scintigraphy determined lesions to be benign in six patients and indeterminate in fourteen patients; however, Na^{18}F PET/CT determined all of these lesions to be malignant.

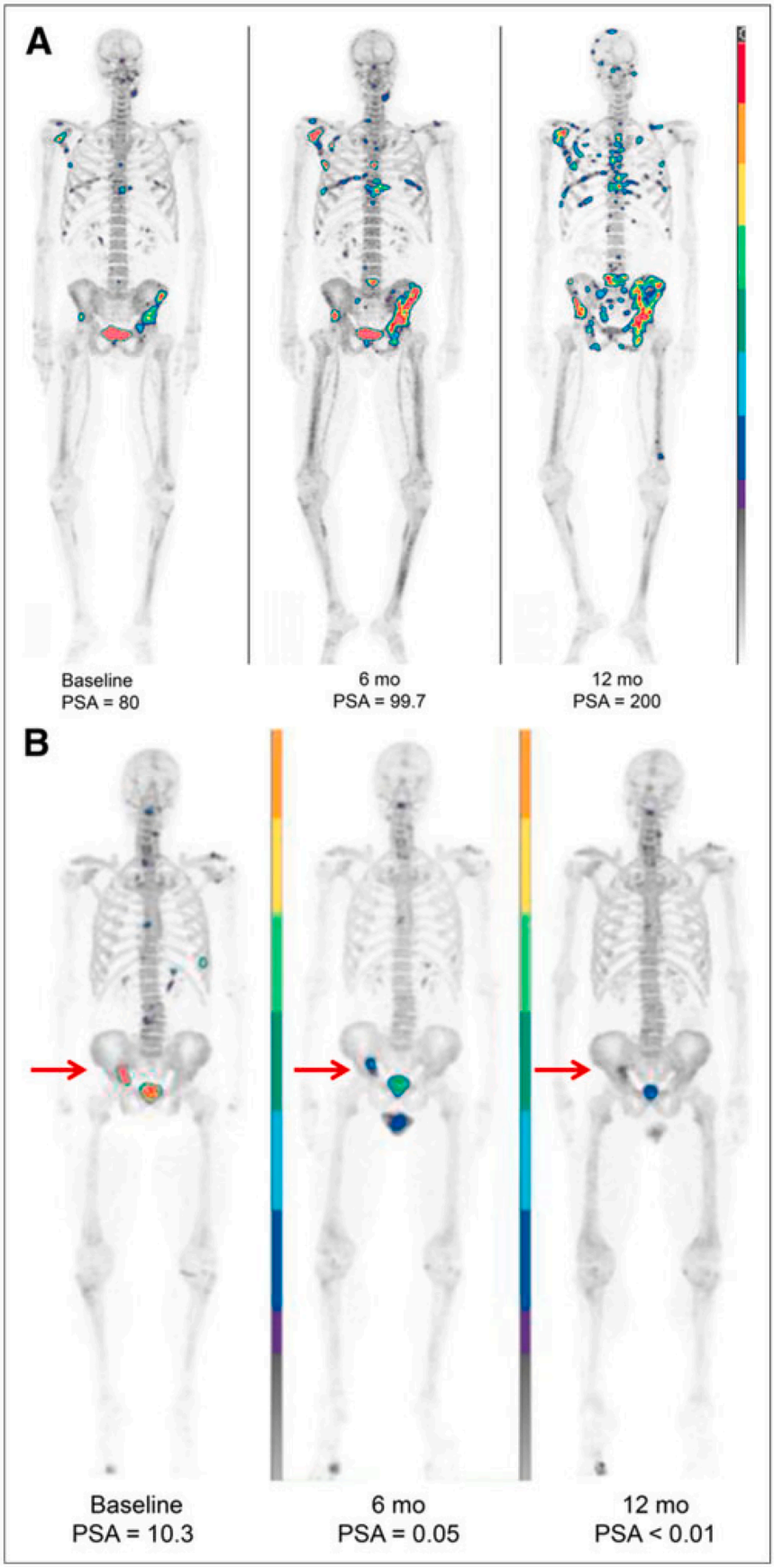

Fig. 3. (A) Progressive disease on $Na^{18}F$ PET/CT in 67-y-old man with postdocetaxel metastatic castration-resistant prostate cancer whose PSA level increased on treatment with abiraterone acetate (6 mo) and cabazitaxel (12 mo). Sequential $Na^{18}F$ PET/CT scans detected multiple new skeletal lesions. Image intensities were equally adjusted.(B) Improved disease on $Na^{18}F$ PET/CT in 66-y-old man with metastatic castration-resistant prostate cancer who had PSA response to docetaxel chemotherapy. Sequential $Na^{18}F$ PET/CT scans showed significant decrease in uptake in right pelvic skeletal lesion. Image intensities were equally adjusted. Originally published in JNM [Ref 28].

Fig. 4. Anterior maximum-intensity projections for both ^{18}F-DCFPyL (A) and Na^{18}F PET/CT (B) demonstrate single bone lesion (arrowheads) suggestive of metastatic disease in right eighth rib. Extensive abnormal uptake in spine on Na^{18}F PET image was attributed to degenerative change by central reviewers. Originally published in JNM [Ref 34].

Additionally, the pre-therapy ^{18}F-NaF PET/CT detected malignant bone lesions in 40 % of the patients who had negative conventional bone scintigraphy, confirming this modality's use for early detection of metastases. A case study example is presented in Fig. 3. Regarding survival, the degree of increased ^{18}F-NaF uptake assessed by standardized uptake value (SUV) was linked with shorter patient survival and a higher risk of death. In essence, there was a significant correlation between the baseline number of malignant lesions and SUV changes in the follow-up ^{18}F-NaF PET/CT scan, and patient survival. These results indicated that ^{18}F-NaF PET/CT is better than the ^{99m}Tc-based tracer in detecting bone metastases, especially early in the course of disease. Along the same lines, Withofs et al compared the accuracy of bone scintigraphy with ^{18}F-NaF PET/CT in detecting bone metastases in breast cancer and prostate cancer patients [29]. Their study demonstrated that ^{18}F-NaF PET/CT was significantly better than bone scintigraphy in detecting bone metastases ($p < 0.0001$). ^{18}F-NaF PET/CT had 76 % sensitivity, 84.2 % specificity, and 80 % accuracy, whereas bone scintigraphy had 44.8 % sensitivity, 79.2 % specificity, and 60 % accuracy. ^{18}F-NaF PET/CT accurately detected metastatic disease in 32 of 33 patients (97 %), with only one false-positive; in contrast, whole-body bone scintigraphy correctly diagnosed 28 of 33 (85 %) patients. This study demonstrates that ^{18}F-NaF is more accurate and sensitive than whole-body bone scintigraphy for detecting bone metastases in breast and prostate cancer patients.

4.2. *Molecular tracers other than ^{18}F-FDG in prostate cancer*

There are other molecular PET tracers that can be complementary or more effective than ^{18}F-FDG as not all cancers are FDG avid [30]. As an example, ^{18}F-FDG-PET has demonstrated low sensitivity in evaluating prostate cancer. Following initial treatment, biochemical recurrence is a significant problem. The ability to determine the extent and location of recurrence is of great relevance for guiding treatment. Choline is a precursor in the synthesis of the phospholipid phosphatidylcholine, which is an important part of the cell wall membrane and is involved in transmembrane signaling. Prostate cancer cells have up-regulated choline kinase, which induces an elevated uptake of choline for synthesis of phospholipids. Once inside the cell, choline is phosphorylated and trapped [31]. ^{11}C-choline and ^{18}F choline (^{18}F-FCH) have been used in a limited fashion in clinical and research studies respectively to detect prostate cancer recurrence.

4.3. *^{11}C-choline PET versus bone scintigraphy in prostate cancer*

Select studies have compared the relevance of ^{11}C-choline PET/CT with bone scintigraphy in detecting bone metastases. In a retrospective analysis involving seventy-eight patients with biochemical progression of prostate cancer, Picchio et al, demonstrated higher specificity of ^{11}C-choline PET/CT for detecting bone metastasis [32]. Furthermore, they found more equivocal findings with bone scintigraphy (^{99m}Tc-MDP) than ^{11}C-choline PET/CT. Garcia et al assessed concordance between ^{11}C-choline PET/CT and bone scan with ^{99m}Tc-HDP for the detection of bone metastases in sixty-two prostate cancer patients [33]. Overall they found good concordance, with ^{11}C-choline detecting more sites of metastatic bone involvement than bone scintigraphy, and bone scintigraphy detecting more benign lesions than PET/CT. Kitajima et al independently compared ^{11}C-choline PET/CT and bone scintigraphy (^{99m}Tc-MDP) for detection of bone metastases in twenty-one patients with prostate cancer [31]. While the sample size is small, they concluded that overall ^{11}C-choline PET/CT had greater sensitivity and accuracy than

bone scintigraphy for detection of bone involvement in patients with prostate cancer. The study highlighted the differences in either tracer uptake due to the osteoblastic or osteoclastic nature of the bone lesion and/or due to the treatment status.

4.4. Prostate-specific membrane antigen (PSMA) PET

A promising strategy to evaluate prostate cancer both at initial diagnosis and recurrence is the radiolabeled prostate-specific membrane antigen (PSMA) such as ^{18}F, ^{68}Ga and ^{99m}Tc PSMA radiotracers. PSMA is a cell surface glycoprotein that exhibits carboxypeptidase and folate hydrolase enzymatic activities. PSMA is expressed at low rates in a normal prostate but is found to be overexpressed in intermediate and high risk primary and metastatic prostate cancers, making it an effective diagnostic and therapeutic biomarker. Bone metastasis is one of the common metastatic sites for prostate cancer, necessitating evaluation of soft tissue and osseous lesions.

Rowe et al compared the sensitivity of PSMA-targeted PET radiotracers (^{18}F-DCFPyl) and ^{18}F-NaF PET in detecting prostate cancer bone metastases respectively (Fig. 4) [34]. The study included a total of sixteen subjects, fifteen of whom were imaged with ^{18}F-DCFPyl followed by ^{18}F-NaF PET. ^{18}F-DCFPyl yielded 96.5 % of bone lesions being definitely positive, 1.0 % being equivocally positive, and 10 % definitely negative. The definitely 10 negative consisted of 80 % sclerotic, 20 % were infiltrative or marrow-based. ^{18}F-NaF PET yielded 95.8 % of bone lesions being definitely positive, 1.0 % equivocally positive and 3.2 % definitely negative. The definitely 10 negative bone lesions on ^{18}F-NaF PET consisted of 92.3 % infiltrative or marrow-based and 7.7 % lytic. For the definitively or equivocally positive lesions, the ^{18}F-DCFPyl median maximum SUV (SUV_{max}) was 7.4 and the ^{18}F-NaF PET SUV_{max} was 18. Ultimately, the sensitivity of ^{18}F-DCFPyl-PET and ^{18}F-NaF PET were almost the same in detection of bone lesions. A benefit of ^{18}F-DCFPyl-PET was in providing additional information about the soft tissue disease.

In another study, Zhang et al compared ^{99m}Tc-PSMA single-photon emission computed tomography (SPECT)/CT with ^{99m}Tc-MDP SPECT/CT in the detection of bone metastasis in prostate cancer [35]. In their study of seventy-four men with pathologically confirmed prostate cancer, ^{99m}Tc-PSMA SPECT/CT and ^{99m}Tc-MDP SPECT/CT scans were performed at an average interval of 12.1 (range, 1–14) days. The proportion of "typical metastasis" versus "equivocal metastasis" during the analysis of bone metastasis detected by the two imaging methods was 26.3:1 (PSMA) and 2.9:1 (MDP) ($P = 0.005$). Furthermore, ^{99m}Tc-PSMA SPECT/CT was superior to ^{99m}Tc-MDP SPECT/CT in the detection of bone metastases in prostate cancer, especially for small lesions and in patients with low PSA levels. In their study, ^{99m}Tc-PSMA SPECT/CT led to a change in management to a more individualized therapy modality for 11 of 74 men (14.9 %).

4.5. ^{18}F-fluciclovine PET for prostate cancer bone metastasis

The intracellular transport of amino acids is upregulated in prostate cancer [36]. Fluorine-18 (^{18}F) fluciclovine (anti-1-amino-3-^{18}F-fluorocyclobutane-1-carboxylic acid (^{18}F-FACBC) is an FDA- and EMA-approved amino acid (leucine) analogue used for imaging recurrent prostate cancer [37]. ^{18}F-FACBC has been successful in visualizing prostate cancer recurrence with bone metastasis, which was missed by conventional CT [38]. ^{18}F-FACBC is transported equally by the sodium-independent L-system and the sodium-dependent ASC (alanine, serine, and cysteine)-system, both of which are linked to aggressive tumor behavior and decreased survival rates. The presence of the tracer in both transport systems implies heavy uptake into tumors with upregulation of the two amino acid transport systems. Bo et al compared the diagnostic performance of Fluciclovine PET/CT and ^{99m}Tc-MDP bone scan in detecting bone metastases in patients with metastatic prostate cancer [39]. In a retrospective study of 106 patients, they showed that sensitivity, specificity, positive predictive value and negative predictive value for bone scan was 79 %, 86 %, 45 % and 96 %, respectively; and 100 %, 98 %, 89 % and 100 % in ^{18}F-fluciclovine PET/CT, respectively. ^{18}F-fluciclovine PET/CT detected more bone metastases than the bone scan and did not miss any lesions detected by the bone scan. A comprehensive review of ^{18}F-fluciclovine PET/CT clinical data is covered by Chau et al. [40]. Overall, Chau et al conclude that the mechanism of uptake action likely confers ^{18}F-fluciclovine superiority over ^{99m}Tc-bone scintigraphy. The superiority is in visualizing cancer lesions in the marrow at early time points as compared to bone scintigraphy that images bone involvement in growing cancer lesions.

5. Molecular imaging in multiple myeloma

In multiple myeloma, molecular imaging of bone marrow is particularly advantageous in staging, detecting minimal residual disease and evaluating response to therapy [41,42]. Molecular PET offers a high degree of specificity for providing molecular and metabolic information in multiple myeloma patients [41]. Advanced hybrid systems such as PET/MRI that combine PET molecular data and MRI functional and anatomic data are highly promising in multiple myeloma. Regardless, ^{18}F-FDG/CT remains the key hybrid modality for multiple myeloma patients.

Multiple myeloma pathogenesis entails the infiltration of malignant monoclonal plasma cells in the bone marrow. Classic imaging techniques such as ^{99m}Tc-MDP bone scintigraphy are not particularly sensitive, making them insufficient in detecting multiple myeloma bone lesions. This is because multiple myeloma lesions are primarily osteolytic [43].

^{18}F-FDG-PET/CT is commonly used for evaluation of multiple myeloma considering its predominantly bone marrow involvement early in the course of disease. Sachpekidis et al evaluated quantitative data on kinetics and distribution patterns of ^{18}F-FDG with regard to pelvic bone marrow plasma cell infiltration in multiple myeloma patients ($n = 52$) [44]. ^{18}F-FDG parameters (SUV_{max}, $SUV_{average}$, K_1, influx, and fractal dimension) were significantly higher ($p < 0.01$) in multiple myeloma lesions in comparison with the reference tissue. PET/CT demonstrated four patterns of uptake: negative, focal, diffuse, and mixed (focal/diffuse). Patients with a mixed pattern of ^{18}F-FDG uptake had the highest mean plasma cell infiltration rate in their bone marrow, whereas those with negative PET/CT demonstrated the lowest bone marrow plasma cell infiltration. There were significant ($p < 0.01$) correlations between focal disease and $SUV_{average}$ ($r = 0.914$), SUV_{max} ($r = 0.790$), and influx ($r = 0.829$) as well as between influx and $SUV_{average}$ ($r = 0.711$). Ultimately, there was significant correlation between ^{18}F-FDG parameters and bone marrow malignant plasma cell infiltration rate.

A recent review by Bezzi et al. [45] evaluated the prognostic value of ^{18}F-FDG-PET/CT in evaluating treatment response and minimal residual disease (MRD), and the possible implications of ^{18}F-FDG-PET/CT in recurrence. Some of the key highlights of this article are: (1) Higher SUV_{max}, more focal bone lesions and extramedullary disease were associated with poor overall survival (OS) and progression-free survival (PFS), (2) Molecular imaging can assist with stratification of patients with stage II and unfavorable prognosis for newer therapies such as immunotherapies, (3) Presence of paramedullary disease [identified by imaging] is associated with lower level of PFS, (4) There is a need for better refinement of PET-quantitative measures such as better thresholding for assessing metabolic tumor volume, (5) There is value in incorporating imaging data together with molecular analyses (such as cfDNA, cpDNA), (6) Normalization of PET/CT after induction and pre-maintenance are positive prognostic factors for PFS and OS, (7) There is complementarity between PET and bone marrow MRD techniques (such as multiparametric flow cytometry approaches, the next generation flow and next generation sequencing) and concordant negativity should be evaluated as a surrogate for outcome prediction.

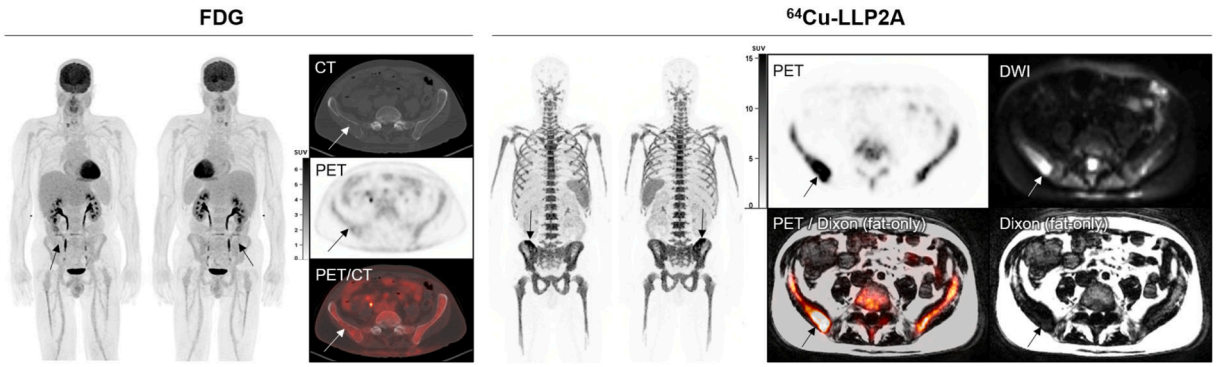

Fig. 5. Multiple myeloma patient underwent PET imaging with ^{64}Cu-LLP2A and ^{18}F-FDG. On PET/CT, an osteolytic lesion in the right iliac bone (arrows) of a multiple myeloma patient had ^{18}F-FDG uptake similar to background marrow. On PET/MRI, this same lesion (arrows) had ^{64}Cu-LLP2A uptake above the background marrow, corresponding to a fat-replacing lesion on fat-only Dixon images and a hyperintense lesion on DWI. In this lesion, the ^{64}Cu-LLP2A SUV-max was 29.5 with an SUL-peak (per PERCIST) of 18.7; in comparison, the ^{18}F-FDG SUV-max was 2.9, with an SUL-peak (per PERCIST) of 2.1. Originally published in JNM [Ref 48].

Finally, given the heterogeneous manifestation of multiple myeloma, there is vibrant interest in developing new and effective molecularly targeted tracers [46]. One such tracer currently under development in the Shokeen and Dehdashti Labs at Washington University is [^{64}Cu]Cu-CB-TE1A1P-LLP2A (^{64}Cu-LLP2A), for imaging the expression of integrin very late antigen-4 (VLA4) (Fig. 5) [47]. Integrin very late antigen-4 (VLA4) is expressed in multiple myeloma cells and pathogenic inflammatory microenvironmental cells, making it a biomarker of interest [48–50]. In a phase I first-in-human study, the tracer was determined to be safe for use in humans [47]. While the optimal use of this tracer will be determined in future Phase II studies, this work demonstrates the potential of imaging markers that interact with the bone and bone marrow microenvironment.

6. Conclusion

Bone metastasis is a common occurrence in metastatic breast and prostate cancer. Metastatic bone lesions severely affect the bone homeostasis, tilting the balance in the favor of tumor cells. This vicious cycle not only leads to pain and complications, but also therapeutic challenges. Nuclear imaging of the bone and bone marrow can hugely benefit patient management by accurately determining the extent of bone involvement and heterogeneity of disease. Specifically the use of bone scintigraphy using bone targeted radioactive molecules and PET imaging using cancer targeted molecular vectors are powerful methods for capturing the spatial distribution, bone involvement and heterogeneity of disease. The select research studies included in this review show the diverse options of imaging methods that are effective at providing information specific to the tumor biology and disease burden.

Declaration of Competing Interest

The authors declare that they have no known competing financial interests or personal relationships that could have appeared to influence the work reported in this paper.

Acknowledgements

This study was supported in-part by R01 CA248493 and R42CA257797. Dr. Shokeen is co-founder of Sarya LLC. Authors declare no other conflict-of-interest.

References

[1] M.S.O. Pijeira, H. Viltres, J. Kozempel, M. Sakmár, M. Vlk, D. İlem-Özdemir, M. Ekinci, S. Srinivasan, A.R. Rajabzadeh, E. Ricci-Junior, L.M.R. Alencar, M. Al Qahtani, R. Santos-Oliveira, Radiolabeled nanomaterials for biomedical applications: radiopharmacy in the era of nanotechnology, EJNMMI Radiopharm. Chem. 7 (2022) 8.
[2] L.B. Solnes, M. Shokeen, N. Pandit-Taskar, Novel Agents and Future Perspectives on Theranostics, Semin. Radiat. Oncol. 31 (2021) 83–92.
[3] R.K. Tahara, T.M. Brewer, R.L. Theriault, N.T. Ueno, Bone Metastasis of Breast Cancer, Adv. Exp. Med. Biol. 1152 (2019) 105–129.
[4] S.H. Park, E.T. Keller, Y. Shiozawa, Bone Marrow Microenvironment as a Regulator and Therapeutic Target for Prostate Cancer Bone Metastasis, Calcif. Tissue Int. 102 (2018) 152–162.
[5] E. Terpos, I. Ntanasis-Stathopoulos, M. Gavriatopoulou, M.A. Dimopoulos, Pathogenesis of bone disease in multiple myeloma: from bench to bedside, Blood Cancer J. 8 (2018) 7.
[6] E. Svensson, C.F. Christiansen, S.P. Ulrichsen, M.R. Rørth, H.T. Sørensen, Survival after bone metastasis by primary cancer type: a Danish population-based cohort study, BMJ Open 7 (2017) e016022.
[7] E. Zamagni, P. Tacchetti, M. Cavo, Imaging in multiple myeloma: How? When? Blood 133 (2019) 644–651.
[8] L. Pang, C. Gan, J. Xu, Y. Jia, J. Chai, R. Huang, A. Li, H. Ge, S. Yu, H. Cheng, Bone Metastasis of Breast Cancer: Molecular Mechanisms and Therapeutic Strategies, Cancers 14 (2022) 5727.
[9] G.J.R. Cook, V. Goh, Molecular Imaging of Bone Metastases and Their Response to Therapy, J. Nucl. Med. 61 (2020) 799–806.
[10] A. Isaac, D. Dalili, D. Dalili, M.A. Weber, State-of-the-art imaging for diagnosis of metastatic bone disease, Radiologe 60 (2020) 1–16.
[11] G.J. O'Sullivan, F.L. Carty, C.G. Cronin, Imaging of bone metastasis: An update, World J. Radiol. 7 (2015) 202–211.
[12] V. Cuccurullo, G.L. Cascini, O. Tamburrini, A. Rotondo, L. Mansi, Bone metastases radiopharmaceuticals: an overview, Curr. Radiopharm. 6 (2013) 41–47.
[13] J. Orcajo-Rincon, J. Muñoz-Langa, J.M. Sepúlveda-Sánchez, G.C. Fernández-Pérez, M. Martínez, E. Noriega-Álvarez, S. Sanz-Viedma, J.C. Vilanova, A. Luna, Review of imaging techniques for evaluating morphological and functional responses to the treatment of bone metastases in prostate and breast cancer, Clin. Transl. Oncol. 24 (2022) 1290–1310.
[14] F. Pesapane, K. Downey, A. Rotili, E. Cassano, D.M. Koh, Imaging diagnosis of metastatic breast cancer, Insights Imaging. 11 (2020) 79.
[15] H.-J. Gallowitsch, E. Kresnik, J. Gasser, G. Kumnig, I. Igerc, P. Mikosch, P. Lind, F-18 Fluorodeoxyglucose Positron-Emission Tomography in the Diagnosis of Tumor Recurrence and Metastases in the Follow-Up of Patients With Breast Carcinoma: A Comparison to Conventional Imaging, Invest. Radiol. 38 (2003) 250–256.
[16] N.Y. Jung, I.R. Yoo, B.J. Kang, S.H. Kim, B.J. Chae, Y.Y. Seo, Clinical significance of FDG-PET/CT at the postoperative surveillance in the breast cancer patients, Breast Cancer 23 (2016) 141–148.
[17] O. Rager, R. Nkoulou, N. Exquis, V. Garibotto, C. Tabouret-Viaud, H. Zaidi, G. Amzalag, S.A. Lee-Felker, T. Zilli, O. Ratib, Whole-Body SPECT/CT versus Planar Bone Scan with Targeted SPECT/CT for Metastatic Workup, Biomed Res. Int. 2017 (2017) 7039406.
[18] S.C. van Es, T. Velleman, S.G. Elias, F. Bensch, A.H. Brouwers, A.W.J. M. Glaudemans, T.C. Kwee, Iersel MW-v, Maduro JH, Oosting SF, de Vries EGE and Schröder CP., Assessment of Bone Lesions with ¹⁸F-FDG PET Compared with ^{99m}Tc Bone Scintigraphy Leads to Clinically Relevant Differences in Metastatic Breast Cancer Management, J. Nucl. Med. 62 (2021) 177–183.
[19] R.L. Bridges, C.R. Wiley, J.C. Christian, A.P. Strohm, An Introduction to Na¹⁸F Bone Scintigraphy: Basic Principles, Advanced Imaging Concepts, and Case Examples, J. Nucl. Med. Technol. 35 (2007) 64–76.
[20] K. Ahuja, H. Sotoudeh, S.J. Galgano, R. Singh, N. Gupta, S. Gaddamanugu, G. Choudhary, ¹⁸F-Sodium Fluoride PET: History, Technical Feasibility, Mechanism of Action, Normal Biodistribution, and Diagnostic Performance in Bone Metastasis Detection Compared with Other Imaging Modalities, J. Nucl. Med. Technol. 48 (2020) 9–16.
[21] C.D. Ramos, (18)F-fluoride PET/CT in clinical practice, Radiol. Bras. (2015;48:Vii-viii.).

[22] L.M. Peterson, J. O'Sullivan, Q.V. Wu, A. Novakova-Jiresova, I. Jenkins, J.H. Lee, A. Shields, S. Montgomery, H.M. Linden, J. Gralow, V.K. Gadi, M. Muzi, P. Kinahan, D. Mankoff, J.M. Specht, Prospective Study of Serial (18)F-FDG PET and (18)F-Fluoride PET to Predict Time to Skeletal-Related Events, Time to Progression, and Survival in Patients with Bone-Dominant Metastatic Breast Cancer, J. Nucl. Med. 59 (2018) 1823–1830.
[23] C.M. Costelloe, H.H. Chuang, J.E. Madewell, N.T. Ueno, Cancer Response Criteria and Bone Metastases: RECIST 1.1, MDA and PERCIST, J. Cancer 1 (2010) 80–92.
[24] G.A. Ulaner, D.M. Hyman, D.S. Ross, A. Corben, S. Chandarlapaty, S. Goldfarb, H. McArthur, J.P. Erinjeri, S.B. Solomon, H. Kolb, S.K. Lyashchenko, J.S. Lewis, J. A. Carrasquillo, Detection of HER2-Positive Metastases in Patients with HER2-Negative Primary Breast Cancer Using 89Zr-Trastuzumab PET/CT, J. Nucl. Med. 57 (2016) 1523–1528.
[25] D.T. Cheng, T.N. Mitchell, A. Zehir, R.H. Shah, R. Benayed, A. Syed, R. Chandramohan, Z.Y. Liu, H.H. Won, S.N. Scott, A.R. Brannon, C. O'Reilly, J. Sadowska, J. Casanova, A. Yannes, J.F. Hechtman, J. Yao, W. Song, D.S. Ross, A. Oultache, S. Dogan, L. Borsu, M. Hameed, K. Nafa, M.E. Arcila, M. Ladanyi, M. F. Berger, Memorial Sloan Kettering-Integrated Mutation Profiling of Actionable Cancer Targets (MSK-IMPACT): A Hybridization Capture-Based Next-Generation Sequencing Clinical Assay for Solid Tumor Molecular Oncology, J. Mol. Diagn. 17 (2015) 251–264.
[26] D.S. Ross, A. Zehir, D.T. Cheng, K. Nafa, G. Jour, P. Razavi, D.M. Hyman, J. Baselga, M.F. Berger, M. Ladanyi, M.E. Arcila, The clinical utility of ERBB2 amplification detection in breast carcinoma using a 341 gene hybrid capture-based next generation sequencing (NGS) assay: Comparison with standard immunohistochemistry (IHC) and Fluorescence In Situ Hybridization (FISH) assays, J. Clin. Oncol. 33 (2015) 604.
[27] P.S.U. Park, W.Y. Raynor, Y. Sun, T.J. Werner, C.S. Rajapakse, A. Alavi, (18)F-Sodium Fluoride PET as a Diagnostic Modality for Metabolic, Autoimmune, and Osteogenic Bone Disorders: Cellular Mechanisms and Clinical Applications, Int. J. Mol. Sci. 22 (2021).
[28] A.B. Apolo, L. Lindenberg, J.H. Shih, E. Mena, J.W. Kim, J.C. Park, A. Alikhani, A. Alikhani, Y.Y. McKinney, J. Weaver, B. Turkbey, H.L. Parnes, L.V. Wood, R. A. Madan, J.L. Gulley, W.L. Dahut, K.A. Kurdziel, P.L. Choyke, Prospective Study Evaluating Na18F PET/CT in Predicting Clinical Outcomes and Survival in Advanced Prostate Cancer, J. Nucl. Med. 57 (2016) 886–892.
[29] N. Withofs, B. Grayet, T. Tancredi, A. Rorive, C. Beckers, G. Jerusalem, R. Hustinx, 18F-Fluoride PET/CT for assessing bone involvement in prostate and breast cancer, J. Nucl. Med. 49 (2008) 21P–P.
[30] K. Shen, B. Liu, X. Zhou, Y. Ji, L. Chen, Q. Wang, W. Xue, The Evolving Role of (18) F-FDG PET/CT in Diagnosis and Prognosis Prediction in Progressive Prostate Cancer, Front. Oncol. 11 (2021), 683793.
[31] K. Kitajima, K. Fukushima, S. Yamamoto, T. Kato, S. Odawara, H. Takaki, M. Fujiwara, K. Yamakado, Y. Nakanishi, A. Kanematsu, M. Nojima, S. Hirota, Diagnostic performance of (11)C-choline PET/CT and bone scintigraphy in the detection of bone metastases in patients with prostate cancer, Nagoya J. Med. Sci. 79 (2017) 387–399.
[32] M. Picchio, E.G. Spinapolice, F. Fallanca, C. Crivellaro, G. Giovacchini, L. Gianolli, C. Messa, [11C]Choline PET/CT detection of bone metastases in patients with PSA progression after primary treatment for prostate cancer: comparison with bone scintigraphy, Eur. J. Nucl. Med. Mol. Imaging 39 (2012) 13–26.
[33] J. Garcia, E. Riera, M. Soler, S. Fuertes, G. Moragas, M. Moragas, I. Carrió, F. Lomeña, Good concordance between 11C-Choline PET-CT and bone scintigraphy for the detection of bone metastases from prostate cancer, J. Nucl. Med. 52 (2011) 38.
[34] S.P. Rowe, X. Li, B.J. Trock, R.A. Werner, S. Frey, M. DiGianvittorio, J.K. Bleiler, D. K. Reyes, R. Abdallah, K.J. Pienta, M.A. Gorin, M.G. Pomper, Prospective Comparison of PET Imaging with PSMA-Targeted (18)F-DCFPyL Versus Na(18)F for Bone Lesion Detection in Patients with Metastatic Prostate Cancer, J. Nucl. Med. 61 (2020) 183–188.
[35] Y. Zhang, Z. Lin, T. Li, Y. Wei, M. Yu, L. Ye, Y. Cai, S. Yang, Y. Zhang, Y. Shi, W. Chen, Head-to-head comparison of 99mTc-PSMA and 99mTc-MDP SPECT/CT in diagnosing prostate cancer bone metastasis: a prospective, comparative imaging trial, Sci. Rep. 12 (2022) 15993.
[36] B. Savir-Baruch, L. Zanoni, D.M. Schuster, Imaging of Prostate Cancer Using Fluciclovine, PET Clinics. 12 (2017) 145–157.
[37] M. Gusman, J.A. Aminsharifi, J.G. Peacock, S.B. Anderson, M.N. Clemenshaw, K. P. Banks, Review of 18F-Fluciclovine PET for Detection of Recurrent Prostate Cancer, Radiographics 39 (2019) 822–841.
[38] P. Nepal, P. Rodrigue, T. Olsavsky, 18F-fluciclovine (Axumin) PET/CT detecting occult bone metastasis, Egypt. J. Radiol. Nucl. Med. 51 (2020) 142.
[39] B. Chen, P. Wei, H.A. Macapinlac, Y. Lu, Comparison of 18F-Fluciclovine PET/CT and 99mTc-MDP bone scan in detection of bone metastasis in prostate cancer, Nucl. Med. Commun. 40 (2019).
[40] A. Chau, P. Gardiner, P.M. Colletti, H. Jadvar, Diagnostic Performance of 18F-Fluciclovine in Detection of Prostate Cancer Bone Metastases, Clin. Nucl. Med. 43 (2018) e226–e231.
[41] R. Vij, K.J. Fowler, M. Shokeen, New Approaches to Molecular Imaging of Multiple Myeloma, J. Nucl. Med. 57 (2016) 1–4.
[42] E.G.M. de Waal, A.W.J.M. Glaudemans, C.P. Schröder, E. Vellenga, R.H.J.A. Slart, Nuclear medicine imaging of multiple myeloma, particularly in the relapsed setting, Eur. J. Nucl. Med. Mol. Imaging 44 (2017) 332–341.
[43] M. Vakili Sadeghi, S. Sedaghat, Is 99m Tc-methylene diphosphonate bone scintigraphy a sensitive method for detecting bone lesions in multiple myeloma? Caspian J. Intern. Med. 9 (2018) 140–143.
[44] C. Sachpekidis, E.K. Mai, H. Goldschmidt, J. Hillengass, D. Hose, L. Pan, U. Haberkorn, A. Dimitrakopoulou-Strauss, (18)F-FDG dynamic PET/CT in patients with multiple myeloma: patterns of tracer uptake and correlation with bone marrow plasma cell infiltration rate, Clin. Nucl. Med. 40 (2015) e300–e307.
[45] D. Bezzi, V. Ambrosini, C. Nanni, Clinical Value of FDG-PET/CT in Multiple Myeloma: An Update, Semin. Nucl. Med. (2022).
[46] J. von Hinten, M. Kircher, A. Dierks, C.H. Pfob, T. Higuchi, M.G. Pomper, S. P. Rowe, A.K. Buck, S. Samnick, R.A. Werner, C. Lapa, Molecular Imaging in Multiple Myeloma—Novel PET Radiotracers Improve Patient Management and Guide Therapy. *Frontiers*, Nuclear Medicine. (2022) 2.
[47] R. Laforest, A. Ghai, T.J. Fraum, R. Oyama, J. Frye, H. Kaemmerer, G. Gaehle, T. Voller, C. Mpoy, B.E. Rogers, M. Fiala, K.I. Shoghi, S. Achilefu, M. Rettig, R. Vij, J.F. DiPersio, S. Schwarz, M. Shokeen, F. Dehdashti, First-in-Human Evaluation of Safety and Dosimetry of (64)Cu-LLP2A for PET Imaging, J. Nucl. Med. (2022).
[48] D. Soodgupta, H. Zhou, W. Beaino, L. Lu, M. Rettig, M. Snee, J. Skeath, J. F. DiPersio, W.J. Akers, R. Laforest, C.J. Anderson, M.H. Tomasson, M. Shokeen, Ex Vivo and In Vivo Evaluation of Overexpressed VLA-4 in Multiple Myeloma Using LLP2A Imaging Agents, J. Nucl. Med. 57 (2016) 640–645.
[49] D. Soodgupta, M.A. Hurchla, M. Jiang, A. Zheleznyak, K.N. Weilbaecher, C. J. Anderson, M.H. Tomasson, M. Shokeen, Very late antigen-4 (α(4)β(1) Integrin) targeted PET imaging of multiple myeloma, PLoS One 8 (2013) e55841.
[50] D. Hathi, C. Chanswangphuwana, N. Cho, F. Fontana, D. Maji, J. Ritchey, J. O'Neal, A. Ghai, K. Duncan, W.J. Akers, M. Fiala, R. Vij, J.F. DiPersio, M. Rettig, M. Shokeen, Ablation of VLA4 in multiple myeloma cells redirects tumor spread and prolongs survival, Sci. Rep. 12 (2022) 30.